Altered balance of inhibitory and active Fc gamma receptors in murine autoimmune glomerulonephritis

Osamu Ichii[1], Akihiro Konno[1], Nobuya Sasaki[2], Daiji Endoh[3], Yoshiharu Hashimoto[1] and Yasuhiro Kon[1]

[1]*Laboratory of Anatomy, Department of Biomedical Sciences, Graduate School of Veterinary Medicine, Hokkaido University, Sapporo, Japan;* [2]*Laboratory of Experimental Animal Science, Department of Disease Control, Graduate School of Veterinary Medicine, Hokkaido University, Sapporo, Japan and* [3]*Department of Veterinary Radiology, School of Veterinary Medicine, Rakuno Gakuen University, Hokkaido, Japan*

***Mag* is an MRL-derived glomerulonephritis susceptibility locus that includes the *Fcgr2b* and *Fcgr3* genes encoding the inhibitory Fc gamma receptor IIB (FcγRIIB) and active FcγRIII, respectively. We measured changes in gene balance in three B6.MRLc1 congenic mouse strains containing the 82-86, 92–100 and 100 cM regions of the MRL chromosome 1. We found that only the strain that has 92-100 (which includes *Fcgr* loci) developed glomerulonephritis. These congenic mice had splenomegaly, elevated blood urea nitrogen, anti-dsDNA antibodies and higher urinary albumin excretion compared to the parental strain C57BL/6(B6). Prior to the development of glomerulonephritis, large CD3- (T cell) and B220- (B cell) positive areas were identified in the spleens of B6.MRLc1(92–100) mice. Both Fc receptors were found in mesangial and dendritic cells; important sites of immune-complex clearance and antigen presentation. The FcγRIII-positive areas were more prominent in the congenic strain. Fcgr2b mRNA was lower in the B6.MRLc1(92–100) kidney and spleen than in those organs of the B6 mice while Fcgr3 expression and the Fcgr3 to Fcgr2b mRNA ratio was higher in the congenic strain kidneys, spleen and thymus than in those of the B6 prior to and at an early stage of glomerulonephritis. We conclude that the imbalance of inhibitory and active Fc gamma receptors influences the pathogenesis of glomerulonephritis.**

Kidney International (2008) **74,** 339–347; doi:10.1038/ki.2008.182; published online 7 May 2008

KEYWORDS: autoimmunity; Fc gamma receptor; glomerulonephritis; kidney; MRL mice

Correspondence: *Yasuhiro Kon, Laboratory of Anatomy, Department of Biomedical Sciences, Graduate School of Veterinary Medicine, Hokkaido University, Kita 18-Nishi 9, Kita-ku, Sapporo 060-0818, Japan.*
E-mail: y-kon@vetmed.hokudai.ac.jp

Received 10 October 2007; revised 5 February 2008; accepted 19 February 2008; published online 7 May 2008

Autoimmune glomerulonephritis (GN) is one of the most severe complications of systemic lupus erythematosus (SLE). Several studies have developed congenic mice derived from autoimmune disease-prone BXSB, NZB, or NZW mice.[1] These studies have clarified that the telomeric region of chromosome 1 (Chr.1) includes several GN-susceptibility loci such as *Bxs3* (71–99 cM), *Sle1* (88 cM), and *Nba2* (92–94 cM).[1] We also created a GN model using B6.MRLc1 (82–100) congenic mice derived from MRL/MpJ widely used as an autoimmune disease model.[2] B6.MRLc1(82–100) has a GN-susceptibility locus termed *MRL autoimmune glomerulonephritis* (*Mag*) that is related with splenomegaly and increased serum autoantibody levels, as well as glomerular damage with immune complex (IC) deposits.[2]

The development and pathological features of GN are strongly affected by glomerular IC depositions.[3–5] The murine Chr.1 (82–100 cM) includes complex genes for the Fcγ-receptor (FcγR) family composed of low-affinity receptors for the Fc region of IgG with a high affinity for ICs.[6,7] The activation of immune responses through mouse FcγR is caused by binding of ICs containing IgG to active FcγRs such as FcγRIII.[6–8] Mouse FcγRIII is encoded by *Fcgr3* localizing on Chr.1 (92.3 cM) and is similar to human FcγRIII in transmembrane/cytoplasmic regions, whereas its extracellular regions show homology to human FcγRII rather than FcγRIII, and this receptor has a common γ-chain linking to immune-receptor tyrosine-based activation motif.[6,7,9,10] On the other hand, these activated immune responses are inhibited by FcγRIIB coded by *Fcgr2b* on Chr.1 (92.3 cM), with an immune-receptor tyrosine-based inhibition motif and high homology to human FcγRIIB.[6,7,11] These FcγRs are prone to bind mouse IgG1- and IgG2-containing ICs rather than IgG3.[6,7]

Recent genome-wide linkage screenings for human SLE have shown significant linkage to Chr.1q23, including the FcγR genes.[12,13] Furthermore, various FcγR-gene polymorphisms affect the pathogenesis of human SLE,[14–16] and some studies have reported that 158-V/F polymorphism in the FcγRIIIA extracellular domain affected IgG binding affinity and was a risk factor for SLE.[17,18] On the other hand, Hatta *et al.*[19] reported that significant differences were detected

between FcγRIIIB-NA1/2 polymorphism and lupus nephritis patients. In animal models, several studies have assessed the role of FcγRs in GN by using FcRγ-chain-deficient mice, mice lacking active FcγRs, or FcγRIIB-deficient mice.[20–23] Briefly, GN of FcRγ-chain-deficient mice with the lupus-prone NZB/W F1 background was ameliorated as compared with that of NZB/W F1 ($\gamma^{+/-}$) mice.[21] In addition, Bolland *et al*. reported that FcγRIIB-deficient mice with a C57BL/6 background exhibited severe GN.[20] From these studies it has been found that the altered physiological functions of inhibitory and active FcγRs appear to have crucial roles in the GN development.

In this study, we generated congenic mice containing the MRL-FcγR-gene locus and demonstrated the altered balance of FcγRIIB and FcγRIII in the kidney and immune organs in this model. Our findings indicate that the imbalance of active and inhibitory FcγRs is closely associated with the pathogenesis of GN and should help in the development of new strategies for diagnosis and therapy targeting these receptors.

RESULTS

MRL-derived congenic strains

Figure 1 illustrates the telomeric region of Chr. 1 and presents the gene names and genetic distances based on the Mouse Genome Database. In the three strains that were produced, only B6.MRLc1(92–100) contains the MRL-derived *Fcgr* locus.

Glomerulonephritis in B6.MRLc1(92–100)

Figure 2 shows light micrographs of the glomerulus from the C57BL/6 and congenic strains. B6.MRLc1(82–86) and B6.MRLc1(100) mice exhibited the normal glomerular structure as C57BL/6 mice (Figure 2a–c). In contrast, B6.MRLc1 (92–100) mice exhibited glomerular damage mainly involving mild cell proliferation at 6 months (Figure 2d). These glomerular lesions had clearly deteriorated with age, and 12-month-old B6.MRLc1(92–100) mice exhibited proliferations of the endothelial and mesangial cells (MCs) and expansion of the mesangial matrix (Figure 2e and f). Certain glomeruli of B6.MRLc1(92–100) mice revealed severe damage with global depositions of periodic acid–Schiff-positive materials and disappearances of capillary and capsular lumina (Figure 2e). Periodic acid-methenamine silver staining revealed membranous lesions such as spike-like alternations

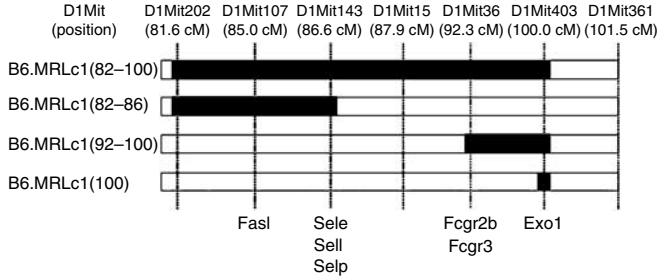

Figure 1 | Representation of the telomeric region of Chr.1 in MRL-derived congenic mice. The upper row shows the B6.MRLc1(82–100) congenic mice produced using *Mag* markers that were reported previously.[2] The three new congenic strains developed in the present study are presented in the subsequent rows: B6.MRLc1(82–86), B6.MRLc1(92–100), and B6.MRLc1(100). The microsatellite markers used for genotyping and their positions (cM) are indicated at the top. The MRL-type congenic intervals are represented by black boxes. Some immune- or cell proliferation-associated genes associated with congenic intervals, such as the Fas ligand (*Fasl*), selectin endothelial (*Sele*), selectin lymphocyte (*Sell*), selectin platelet (*Selp*), Fcγ receptor (*Fcgr*), and exonuclease1 (*Exo1*), are indicated at the bottom.

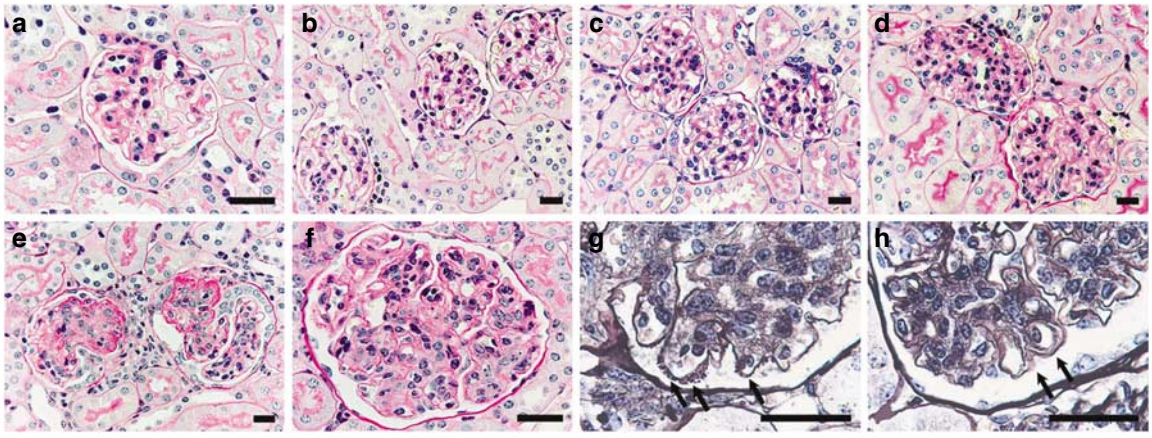

Figure 2 | Light micrographs of the renal cortices from C57BL/6 and MRL-derived congenic mice. Twelve-month-old female C57BL/6 mice (**a**), 8-month-old female B6.MRLc1(82–86) mice (**b**), 8-month-old female B6.MRLc1(100) mice (**b**), 6-month-old female B6.MRLc1 (92–100) mice (**d**), 12-month-old female B6.MRLc1(92–100) mice (**e**–**h**). B6.MRLc1(82–86) and B6.MRLc1(100) mice have normal renal structures similar to C57BL/6 mice, and their glomeruli present no histopathological changes (**a**–**c**). B6.MRLc1(92–100) mice exhibit proliferative glomerular lesions that mainly comprise proliferation of mesangial cells and expansion of mesangial matrices, and these lesions deteriorate with age (**d**–**f**). Glomeruli of B6.MRLc1(92–100) mice at 12 months reveal membranous lesions such as thickening of the glomerular basement membrane, spike-like alternations, and a double contour of glomerular basement membrane (arrows, **g**, **h**). Certain glomeruli of B6.MRLc1(92–100) mice exhibit global deposition of periodic acid–Schiff-positive material and disappearance of capillary and capsular lumina (**e**). Periodic acid–Schiff- (**a**–**f**) and periodic acid–methenamine silver-stained (**g**, **h**) cortices. Bars = 20 μm.

or double contour of glomerular basement membranes in 12-month-old B6.MRLc1(92–100) mice (Figure 2g and h).

Immunofluorescence revealed glomerular IgG-containing IC deposits in B6.MRLc1(92–100) mice (Figure 3). IgG1- and IgG2b-positive reactions were mainly observed in the glomerular mesangial regions of B6.MRLc1(92–100) mice; however, these reactions were considerably few in the C57BL/6 strain.

The glomerular damage in the B6.MRLc1(92–100) strain was also assessed histometrically (Figure 4a and b). Briefly, at 6 and 12 months of age, that is, at the early and late GN development stages reported for B6.MRLc1(82–100) mice,[2] the diameter of the renal corpuscle and the numbers of nuclei in the glomeruli were measured as indices for the degree of glomerular hypertrophy and proliferative lesions, respectively. B6.MRLc1(92–100) mice had significantly higher values of renal corpuscle diameter than mice of the C57BL/6 strain, at 12 months (Figure 4a), and the numbers of nuclei in glomeruli was high in B6.MRLc1(92–100) mice at both ages (Figure 4b).

Measurement of serum creatinine and blood urea nitrogen level and urinary albumin detection were performed for 6- and 12-month-old mice. No significant differences were observed in creatinine levels, but B6.MRLc1(92–100) mice tended to show higher values than C57BL/6 mice at 12 months of age (Figure 4c). B6.MRLc1(92–100) mice had higher blood urea nitrogen levels than C57BL/6 at both ages, and significant differences were observed at 12 months of age (Figure 4d). Albumin was detected in the urine samples by sodium dodecyl sulfate (SDS)-polyacrylamide gel electrophoresis. Using bovine serum albumin as the control, the urine protein fraction of approximately 66 kDa was determined to be the albumin fraction. The albumin band was identified in both the strains; however, B6.MRLc1(92–100) mice, especially at 12 months, exhibited strong albumin excretions as compared with C57BL/6 mice (Figure 4e).

Activation of immune system in B6.MRLc1(92–100) mice

Figure 5a and b shows the spleen weights and serum levels of anti-double-stranded DNA (dsDNA) antibodies (Abs) of C57BL/6 and B6.MRLc1(92–100) mice at 6 and 12 months of age, respectively. B6.MRLc1(92–100) mice exhibited significantly higher values of spleen weights at 12 months of age than C57BL/6 mice and also had higher serum levels of anti-dsDNA Abs at both 6 and 12 months of age.

Figure 5c–f illustrates the immunohistochemistry for CD3 (T-cell marker) and B220 (B-cell marker) at 1 month when no histological renal changes were observed in B6.MRLc1(92–100) mice. CD3- and B220-positive areas were observed in the periarteriolar lymphatic sheath and splenic

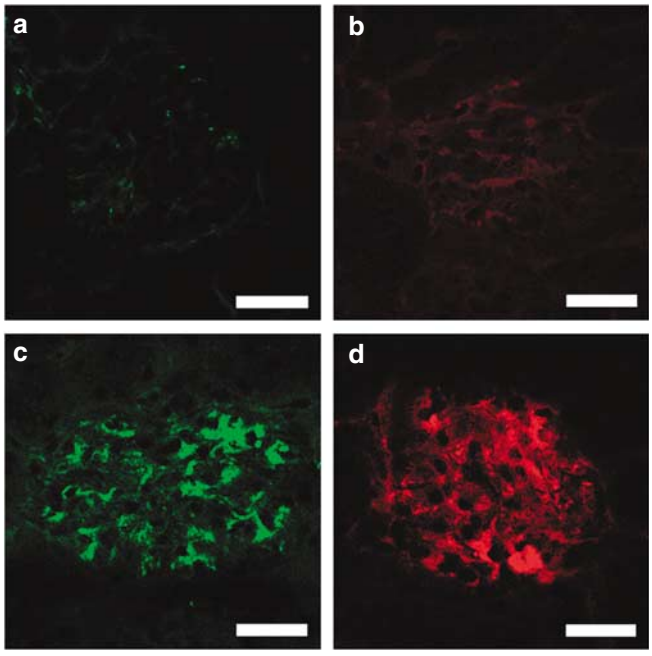

Figure 3 | Direct immunofluorescence on cryostat sections for detecting IgG subtypes in glomeruli from 6-month-old C57BL/6 and B6.MRLc1(92–100) mice. The sections were analyzed by confocal microscopy. IgG1-positive reactions are visualized using FITC-conjugated antibodies (green, **a**, **c**). IgG2b-positive reactions are visualized using tetramethyl rhodamine isothiocyanate-conjugated antibodies (red, **b**, **d**). Clear immunoreactions of IgG1 and IgG2b are observed in the mesangial regions of a 6-month-old B6.MRLc1(92–100) mouse (**c**, **d**); however, these reactions are very weak in corresponding C57BL/6 mice of the same age (**a**, **b**). Bars = 20 μm.

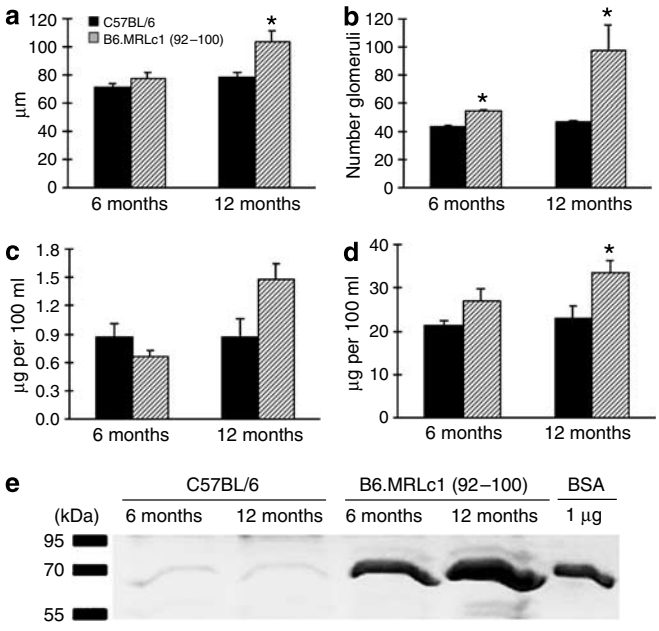

Figure 4 | Comparison of the indices for GN between C57BL/6 and B6.MRLc1(92–100) mice at 6 and 12 months of age. (**a**) Diameter of the renal corpuscle. (**b**) Number of nuclei present in the glomeruli. (**c**) Serum levels of creatinine. (**d**) Serum levels of blood urea nitrogen. Each value represents the mean ± s.e. * Significantly different from C57BL/6 mice of the same age (Mann–Whitney *U*-test, $P < 0.05$); $n \geqslant 3$. (**e**) Detection of urinary albumin. We analyzed 3 μl of urine from C57BL/6 and B6.MRLc1(92–100) mice by SDS-polyacrylamide gel electrophoresis. As control, 1 μg of bovine serum albumin was used.

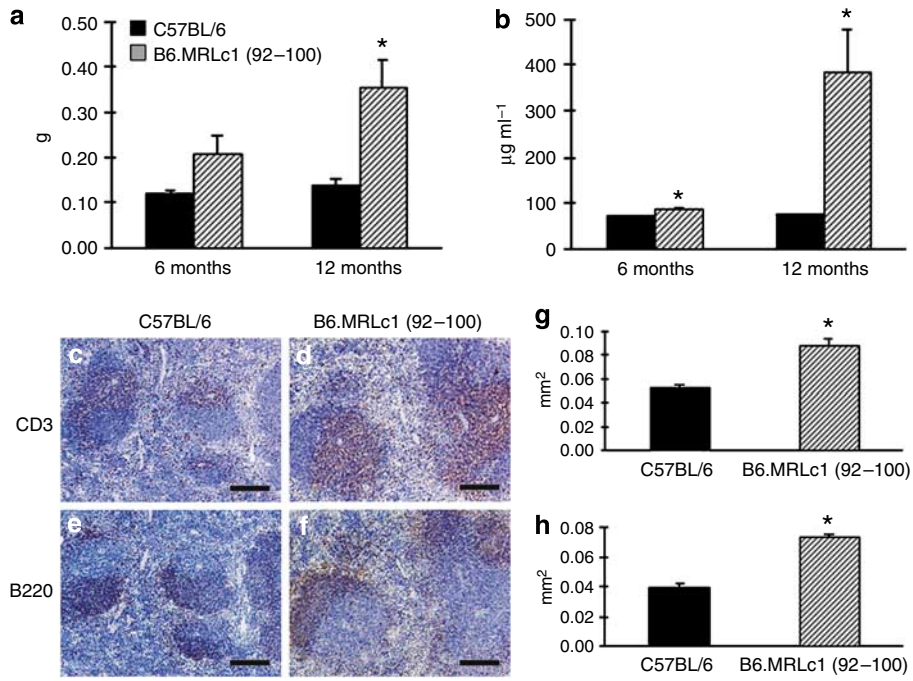

Figure 5 | Comparisons of the indices for development of autoimmune disease between C57BL/6 and B6.MRLc1(92–100) mice. (**a**) Spleen weight. (**b**) Serum levels of anti-dsDNA antibody. Each value represents the mean ± s.e. * Significantly different from C57BL/6 mice of the same age (Mann–Whitney *U*-test, $P < 0.05$); $n \geqslant 3$. (**c**–**f**) Immunohistochemical detection of CD3- and B220-positive cell areas in spleens obtained from 1-month-old C57BL/6 and B6.MRLc1(92–100) mice. CD3- and B220-positive areas were mainly observed in the periarteriolar lymphatic sheath and splenic lymphoid follicles, respectively. Notably, both CD3- and B220-positive cell areas in B6.MRLc1(92–100) mice (**d**, **f**) are more widely observed than in C57BL/6 mice (**c**, **e**). Bars = 100 μm. (**g**, **h**) Histometric analysis for CD3- and B220-positive areas in spleens at 1 month of age. Each value represents the mean ± s.e. * Significantly different from C57BL/6 (Mann–Whitney *U*-test, $P < 0.05$) mice; $n \geqslant 5$.

lymphoid follicles, respectively. Spleen weights of both the strains did not differ significantly at 1 month of age (C57BL/6: 49 ± 0.4 mg and B6.MRLc1(92–100): 52 ± 0.2 mg), whereas these immune-positive areas were more widely observed in B6.MRLc1(92–100) than in C57BL/6 mice (Figure 5 c–e). These observations were confirmed by histometric analysis for measurement of CD3- and B220-positive areas in the spleen. B6.MRLc1(92–100) mice had significantly higher values of each parameter than C57BL/6 mice (Figure 5g and h).

Localizations of FcγRs

In the kidney, FcγR-positive reactions were mainly observed in the glomerular mesangial regions in both C57BL/6 and B6.MRLc1(92–100) mice (Figure 6a, b, g, and h). Interestingly, although intensity of FcγRIIB-positive reactions was similar among strains (Figure 6a and g), FcγRIII-positive reactions were strongly observed in B6.MRLc1(92–100) mice (Figure 6b and h). In the spleen, reticular FcγR-positive reactions were mainly observed in the germinal centers of splenic lymphoid follicles, and these reactions morphologically appeared to represent the cytoplasmic processes of dendritic cells (DCs) (Figure 6c, d, i, and j). Indeed, double staining for FcγRIII and CD11c used as the DC markers demonstrated colocalization of these materials (Figure 7a). Similar to those in the kidney, FcγRIII-positive reactions in splenic lymphoid follicles were stronger in B6.MRLc1 (92–100) mice (Figure 6d and j). In the thymus, FcγRIIB-positive reactions represented a single cell that was localized at the boundary between the thymic cortex and medulla (Figure 6e and k), and the reaction intensities were similar among strains. On the other hand, FcγRIII-positive cells could only be detected in B6.MRLc1(92–100) mice, and the morphological features of these cells were similar to FcγRIIB-positive cells that had elliptic nuclei and processed cytoplasm (Figure 6e, k, and l). In the double staining for FcγRIII and CD11c, these localizations appeared to be were fused and merged yellow (Figure 7b).

mRNA expressions of *Fcgrs*

Figure 8 shows the mRNA expressions of the FcγR genes and β-*actin* in the kidney, spleen, and thymus of B6.MRLc1 (92–100) and C57BL/6 at mice 1 month. *Fcgr2b* expression was observed in three organs in both the strains, and no difference in the expression intensity was observed among strains (Figure 8, upper lane). On the other hand, although *Fcgr3* expression was also detected in three organs of both the strains, the intensity of expression was stronger in B6.MRLc1(92–100) and weaker in C57BL/6 mice.

Figure 9 shows the results of quantitative real-time PCR analysis for relative *Fcgr2b* and *Fcgr3* mRNA expression levels in the kidney, spleen, and thymus at the non-GN development stage (1 month) and early GN development stage

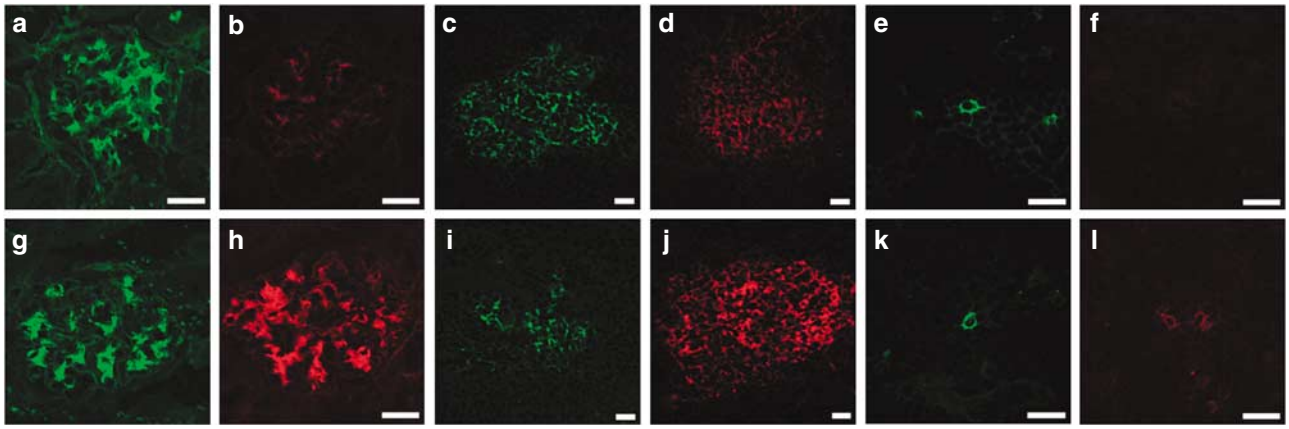

Figure 6 | Indirect immunofluorescence on cryostat sections for the detection of FcγIIB and FcγRIII in 6-month-old mice. Kidney (**a**, **b**, **g**, **h**), spleen (**c**, **d**, **i**, **j**), and thymus (**e**, **f**, **k**, **l**). The sections are analyzed by confocal microscopy. FcγRIIB-positive reactions are visualized using an anti-mouse FcγRIIB primary antibody and FITC-conjugated secondary antibody (green, **a**, **g**, **c**, **i**, **e**, **h**). FcγRIII-positive reactions are visualized using an anti-mouse FcγRIII primary antibody and tetramethyl rhodamine isothiocyanate-conjugated secondary antibody (red, **b**, **h**, **d**, **j**, **f**, **l**). In the kidney, FcγRIIB-positive and FcγRIII-positive reactions are observed in the glomerular mesangial regions in C57BL/6 (**a**, **b**) and B6.MRLc1(92–100) mice (**g**, **h**), and the intensity of the FcγRIII-positive reaction in B6.MRLc1(92–100) mice (**h**) is stronger than that in C57BL/6 mice (**b**). In the spleen, reticular FcγRIIB- and FcγRIII-positive reactions are observed in the germinal centers of the splenic lymph follicles in C57BL/6 (**c**, **d**) and B6.MRLc1(92–100) mice (**i**, **j**), and the intensity of FcγRIII-positive reactions in B6.MRLc1(92–100) mice (**j**) is stronger than that in C57BL/6 mice (**d**). In the thymus, FcγRIIB-positive reactions represent a single cell that localized on the boundary between the thymic cortex and medulla, and has elliptic nuclei and processed cytoplasm (**e**, **k**). FcγRIII-positive cells are observed in B6.MRLc1(92–100) mice exclusively and the morphological features of these cells resemble those of FcγRIIB-positive cells (**l**). Bars = 20 μm.

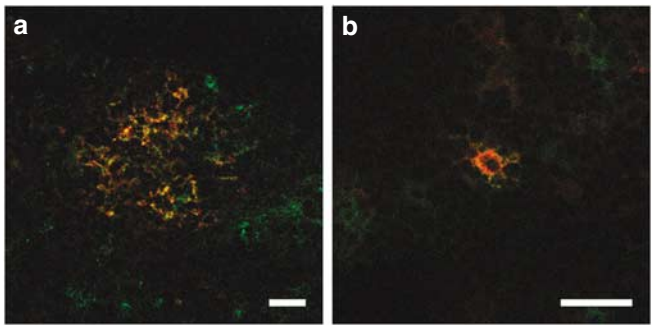

Figure 7 | Double immunofluorescence on cryostat sections for detection of CD11c and FcγRIII in 6-month-old B6.MRLc1(92–100) mice. Spleen (**a**) and thymus (**b**). The sections are analyzed by confocal microscopy. CD11c-positive reactions are visualized using an anti-mouse CD11c primary antibody and FITC-conjugated secondary antibody (green). FcγRIII-positive reactions are visualized using an anti-mouse FcγRIII primary antibody and tetramethyl rhodamine isothiocyanate-conjugated secondary antibody (red). In spleen, reticular CD11c-positive and FcγRIII-positive reactions are shown to be colocalized (yellow, **a**). In the thymus, the immune-positive reactions of FcγRIII and CD11c are fused in a cell having processed cytoplasm (yellow, **b**). Bars = 20 μm.

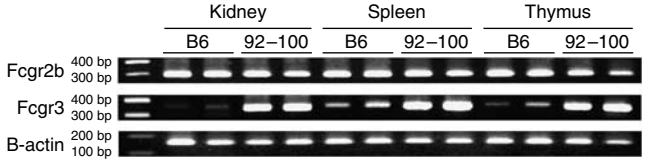

Figure 8 | Reverse transcriptase-PCR analysis for *Fcgr2b*, *Fcgr3*, and β-*actin* mRNA expression in the kidney, spleen, and thymus of 6-month-old B6.MRLc1(92–100) and C57BL/6 mice. Upper lane (*Fcgr2b*), middle lane (*Fcgr3*), and bottom lane (β-*actin*). Size markers are represented on the left ($n = 2$).

(6 months). At 1 month, *Fcgr2b* levels in the kidney and spleen were significantly lower in B6.MRLc1(92–100) than in C57BL/6 (Figure 9a) mice. In contrast, the *Fcgr3* levels in the three organs were significantly higher in B6.MRLc1(92–100) than in C57BL/6 (Figure 9b) mice. At 6 months, *Fcgr2b* levels in the kidney and spleen tended to be lower in B6.MRLc1 (92–100) than in C57BL/6 mice; however, the reverse was true in the case of the thymus (Figure 9c). On the other hand, *Fcgr3* levels in three organs were significantly higher in B6.MRLc1(92–100) than in C57BL/6 (Figure 9d) mice.

Figure 10 shows the ratio of relative mRNA expression of *Fcgr3* to that of *Fcgr2b* in 1- and 6-month-old B6.MRLc1 (92–100) and C57BL/6 mice. The values are expressed as fold increases as compared with those in C57BL/6 mice. At 1 month, B6.MRLc1(92–100) mice exhibited higher values than C57BL/6 in three organs, with the largest difference in the thymus (Figure 10a). At 6 months, a similar tendency was observed for three organs, and the values in B6.MRLc1 (92–100) mice were markedly higher than those in C57BL/6 mice in the kidney and spleen (Figure 10b).

DISCUSSION

MRL-Chr. 1 (82–100 cM) includes GN-susceptibility locus termed *Mag*.[2] In this study, we produced three congenic strains including *Mag* regions (82–86, 92–100, 100 cM) to confirm the contributions of the FcγR-gene locus to GN development. Previous studies have demonstrated that *Fasl*

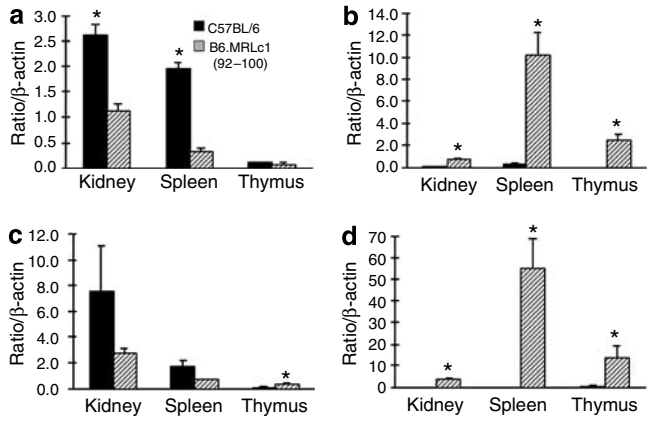

Figure 9 | Comparison of relative *Fcgr2b* and *Fcgr3* mRNA expression in the kidney, spleen, and thymus among 1- and 6-month-old B6.MRLc1(92–100) and C57BL/6 mice by quantitative real-time PCR analysis. (**a**) *Fcgr2b* at 1 month of age. (**b**) *Fcgr3* at 1 month of age. (**c**) *Fcgr2b* at 6 months of age. (**d**) *Fcgr3* at 6 months of age. Each value of *Fcgr2b* and *Fcgr3* is normalized by that of β-*actin* and represents the mean ± s.e. *Significantly different from C57BL/6 mice (Mann–Whitney *U*-test, $P < 0.05$); $n \geqslant 3$.

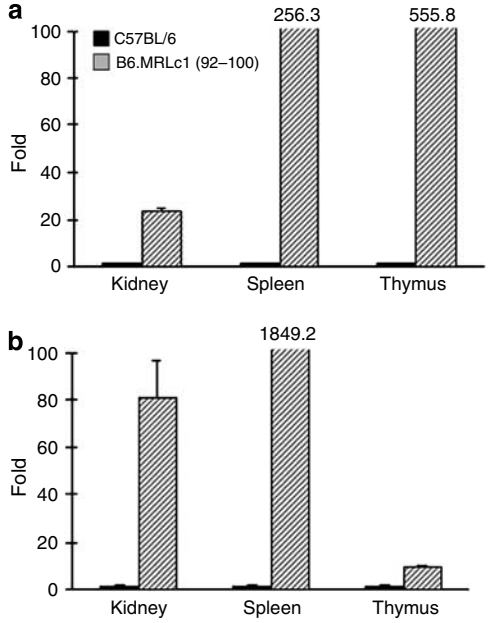

Figure 10 | The ratios of relative mRNA expression of *Fcgr3* to that of *Fcgr2b* in 1- and 6-month-old B6.MRLc1(92–100) and C57BL/6 mice. (**a**) 1 month of age. (**b**) 6 months of age. Raw values of *Fcgr2b* and *Fcgr3* are normalized by that of β-*actin* and are expressed as fold increases compared with C57BL/6 mice. Each value represents the mean ± s.e. ($n \geqslant 3$).

(85.0 cM) deficiencies mediating apoptosis and the *selectin* family (86.6 cM) relating to cellular adhesion led to GN in the autoimmune disease-prone mouse.[24,25] Furthermore, *Exo1* (100 cM), which is involved in DNA repair, was suggested as a candidate gene for testicular apoptosis in MRL/MpJ.[26] However, histopathological examinations demonstrated that only B6.MRLc1(92–100) exhibited glomerular damage. In addition, B6.MRLc1(92–100) mice revealed glomerular IC depositions, slight aggravation of renal function, and increased spleen weights and autoantibody levels. From these findings, it was clarified that B6.MRLc1(92–100) mice had autoimmunity-mediated glomerular damage and confirmed that MRL-Chr.1 (92.3–100 cM), including the FcγR-gene locus, but not other *Mag* regions such as *Fasl*, *selectin* family, or *Exo1*, was crucial for development of GN.

In this study, FcγR-positive reactions were observed in the glomerular mesangial regions. Glomerular MCs participate in the regulation of glomerular filtration rate and in glomerular pathogenesis.[27,28] Activated MCs produce various inflammatory mediators [29,30] Radeke *et al.*[31] demonstrated that normal murine MCs mainly expressed FcγRII rather than FcγRIII, and that stimulation, such as interferon-γ, caused downregulation of FcγRII, with activation of FcγRIII, inducing production of chemokines such as monocyte chemoattractant protein-1 in MCs. Our results were consistent with these reports: B6.MRLc1(92–100) exhibited stronger FcγRIII-positive reactions than C57BL/6 mice, and *Fcgr2b* downregulation and *Fcgr3* upregulation were observed in the kidneys. From these findings, it was considered that the altered balance of FcγRs in MCs might contribute to the pathogenesis of GN in B6.MRLc1(92–100) mice through alterations in the conditions of local glomerular chemokine or cytokine production.

In the spleen and thymus, FcγR-positive cells were identified as DCs by immunofluorescence. Similar to that observed in the kidney, B6.MRLc1(92–100) mice had stronger FcγRIII-positive reactions and higher *Fcgr3* to *Fcgr2b* ratios as compared with C57BL/6 mice in these organs. Recent studies suggested that FcγRs on DCs mediate phagocytosis and antigen presentation associated with maturation of DCs and stimulation of T cells.[32,33] Desai *et al.*[32] suggested that FcγRIIB was required for peripheral tolerance through inhibition of DC activation or limiting antigen processing. Furthermore, Boruchov *et al.*[34] demonstrated that the altered balances of inhibitory and active FcγRs in human DCs induced production of cytokines such as tumor-necrosis factor-α, and concluded that coexpression of these FcγRs in DCs was associated with tolerance or immunity by ICs. Interestingly, in the kidney, MCs had immunological functions similar to DCs, and it was suggested that activated MCs expressed major histocompatibility complex-II and intercellular adhesion molecule-1, and could function as antigen-presenting cells, and that they directly contacted lymphocytes.[35,36] Therefore, the altered balance of FcγRs in immunological principal-function units, such as DCs or MCs, may contribute to the pathogenesis of GN by causing disruption of immune functions such as antigen presentation or IC clearance through over-activation of these cells.

Interestingly, from the results of immunohistochemistry for CD3 and B220, it was suggested that activation of immune system in B6.MRLc1(92–100) mice was caused before development od GN. Furthermore, in the non-GN

development stage, the balance of *Fcgr* expressions was clearly altered in the immune organs of B6.MRLc1(92–100) mice. Previous studies have reported the role of FcγRIIB in the negative selection of lymphocytes and suggested that B cells expressed FcγRIIB, and hypermutated B cells were eliminated by FcγRIIB-dependent apoptosis triggered by DC-bound ICs.[6] In addition, Durum *et al.*[37] reported that FcγRIII on embryonic thymocytes played an important role in T-cell development, on the basis of data demonstrating that anti-FcγRIII Abs treatment blocked rearrangement of the T-cell receptor-β locus and T-cell development. Although we could not assess the interactions between FcγRs and lymphocytes, the relationships between the functional deficiency of FcγRs in the juvenile period and the production of autoreactive lymphocytes might be associated with the innate autoimmune disease-prone trait.

Recently, *Fcgr2b* promoter-region polymorphisms, which cause a reduction in the gene transcription, were reported in autoimmune disease-prone strains, including MRL.[38] Furthermore, a recent study suggested that some SLE patients exhibited decreased FcγRIIB-gene transcriptions mediated by −343 G/C promoter-region polymorphism.[39] Indeed, *Fcgr2b* levels were lower in B6.MRLc1(92–100) than in C57BL/6 mice in the non-GN development stage. Therefore, it was considered that one of the causes of *Fcgr* imbalances was *Fcgr2b* promoter-region polymorphism. However, *Fcgr3* upregulation was more severe than *Fcgr2b* downregulation in B6.MRLc1(92–100) mice. Clynes *et al.*[21] reported that in FcRγ-chain-deficient mice with a GN-prone background, lacking active FcγRs, glomerular inflammation was prevented; however, the amount of glomerular IC depositions was not altered. Fujii *et al.*[40] suggested that FcγRIII-deficient mice exhibited resistance to anti-glomerular basement membrane GN, and FcγRIII played a predominant role in the induction of glomerular damage. From these findings, it can be stated that FcγRIII activation is ultimately essential for the glomerular inflammatory cascade in murine GN. However, the apparent contradiction exists between the human and mouse concerning the role of FcγRIII in GN. The more functional form of FcγRIII would be expected to promote autoimmune GN in mouse, whereas the less functional form is associated with human SLE. Briefly, it was suggested that FcγRIIIA 158-V/F polymorphism, especially 158-F allele, which caused decrease of IC-binding ability, was linked to the development of human SLE.[17,18] On the basis of these findings, in murine GN models, the changes in the FcγR balances, rather than those in the IC-binding ability, can be said to have a great impact on the development of GN.

The murine Chr.1 (92–100 cM) contains not only FcγR genes but also other immune- and cell proliferation-associated genes. *Crp* (94.2 cM) and *Apcs* (94.2 cM) code C-reactive protein and serum amyloid P component. Interestingly, it has been suggested that C-reactive protein and serum amyloid P component recognize ligands from apoptotic cells, bind to FcγRs, and play important roles in presentation and clearance of self-antigen.[41] Furthermore, it was reported that serum amyloid P component-deficient mice developed GN and that C-reactive protein administration to NZB/W F1 induced their prolonged survival and decreased autoantibody levels.[42,43] On the other hand, it was reported that the *Ifi202* (95.2 cM) promoter-region polymorphism correlated with the contribution of *Nba2* to lupus, and MRL has a polymorphism in this region similar to that of NZB.[44,45] Thus, not only FcγR genes, but also other genes in Chr.1 (92–100 cM), might be associated as initiators or accelerators with GN of B6.MRLc1(92–100) mice.

In conclusion, we demonstrated that B6.MRLc1(92–100) mice having the MRL-FcγR-gene locus clearly presented with GN. It was clarified that the balance of inhibitory FcγRIIB and active FcγRIII, localizing glomerular mesangial regions and DCs, was remarkably altered in the kidney and immune organs of B6.MRLc1(92–100) mice. We propose that the imbalances of inhibitory and active FcγRs hold a key in elucidating the pathogenesis of GN.

MATERIALS AND METHODS

Generation of congenic mice

B6.MRLc1(82–100) were generated as reported by Ichii *et al.*,[2] and C57BL/6 were purchased from an animal-breeding company (Japan SLC Inc., Hamamatsu, Japan) and maintained under conventional conditions. For care and handling of experimental animal, the investigators adhered to the 'Guide for the Care and Use of Animals' by the School of Veterinary Medicine, Hokkaido University. The F1 generation was produced by crossing C57BL/6 with B6.MRLc1(82–100) mice and backcrossed with C57BL/6 mice to produce the N2 generations. N2 animals were typed for six microsatellite markers D1mit202–403 (Figure 1). The map positions of the microsatellite loci were based on the Mouse Genome Database. Polymorphisms between congenic strains and C57BL/6 were detected by a PCR-based method.[2] Heterozygotes for three regions (81.6–86.6, 92.3–100, and 100 cM) were bred to C57BL/6 mice to produce N3 generations. Finally, three MRL-type homozygous mice designated B6.MRLc1(82–86, 92–100, and 100) were created and maintained from 5 to 10 generations by further inbreeding and were used in the experiments.

Tissue preparation for histological studies

Under deep anesthesia, mice were killed by exsanguination from carotid arteries, and the kidneys, spleens, and thymuses were immediately removed at 1–12 months. A part of each sample was fixed in 10% formalin at room temperature for histopathological analysis and immunohistochemistry. The remaining part was frozen in liquid nitrogen after OCT compound embedding (Tissue-tek; Sakura Finetek, Torrance, CA, USA) and stored at −80 °C for immunofluorescence.

Histopathological analysis

To assess the severity of glomerular damage, paraffin sections (2 μm) from 6- and 12-month-old mice were stained with periodic acid–Schiff. Digital images of 30 glomeruli per kidney were prepared and the number of nuclei per glomerulus and the diameters of renal corpuscles were measured using Adobe Photoshop version 6.0 (Mountain View, CA, USA). A part of the paraffin sections obtained from 12-month-old mice was stained with periodic acid–methenamine silver for detection of membranous lesions.

Immunohistochemistry

Immunohistochemistry for CD3 and B220 in the spleen paraffin sections was performed using unlabeled rabbit anti-CD3 Ab (Dako, Kyoto, Japan) and rat anti-B220 Ab (Cedarlane Laboratories, Homby, Ontario, Canada), as described previously.[2] The CD3- and B220-positive areas in the spleen sections were measured in 1-month-old mice. Briefly, using ImageJ version 1.32j (NIH, Bethesda, MD, USA), more than 35 CD3- or B220-positive absolute areas per animal were measured on digital images of spleen obtained with a digital camera, and the mean of each area was compared between C57BL/6 and B6.MRLc1(92–100) mice.

Immunofluorescence

We treated 4-μm thick cryosections with goat fluorescein isothiocyanate (FITC)-labeled anti-IgG1 Ab and tetramethyl rhodamine isothiocyanate-labeled anti-IgG2b Ab (Caltag Laboratories, South San Francisco, CA, USA) diluted to 1:100 for 2 h at room temperature. Further, the cryosections were treated with unlabeled rat anti-FcγRIIB Ab and goat anti-FcγRIII Abs (R&D Systems, Minneapolis, MN, USA) diluted to 1:200 for 2 h at room temperature. The FcγRIIB and FcγRIII sections were incubated with undiluted FITC-conjugated goat anti-rat IgG Ab and tetramethyl rhodamine isothiocyanate-conjugated rabbit anti-goat IgG Ab (Zymed, South San Francisco, CA, USA), respectively, diluted to 1:100. For double staining for FcγRIII and CD11c, sections were incubated with hamster anti-CD11c Ab (Chemicon, Temecula, CA, USA) diluted to 1:200 and FITC-conjugated rabbit anti-hamster Ab (Southern Biotechnology Association, Birmingham, AL, USA) diluted to 1:100 according to the same protocol as that used for FcγRs after the FcγRIII-staining procedure. These sections were examined by confocal microscopy.

Serological analysis and urinalysis

The serum levels of creatinine, blood urea nitrogen, and anti-dsDNA Abs were determined using BUN-test-Wako (Wako Pure Chemical Industries, Osaka, Japan), the Creatinine Assay kit (Cayman Chemical, Ann Arbor, MI, USA), and the mouse anti-dsDNA Ab ELISA kit (Alpha Diagnostic International, San Antonio, TX, USA) according to the manufacturer's directions. Urinary albumin was detected by SDS-polyacrylamide-gel electrophoresis. We heated 3 μl of urine and 1 μg of bovine serum albumin at 65 °C for 5 min in 2 × SDS sample buffer (100 mM Tris-HCl, pH 6.8, 20% glycerol, 4% SDS, 0.02% bromophenol blue, 12% 2-mercaptoethanol) and loaded on 12% polyacrylamide gel (e-PAGEL; ATTO Corporation, Tokyo, Japan). Electrophoresis was performed at 150 V in Tris-glycine buffer (25 mM Tris, pH 8.3, 192 mM glycine) containing 0.1% SDS for 2 h. Gels were stained with Quick CBB PLUS (Wako Pure Chemical Industries).

Reverse transcriptase-PCR and quantitative real-time PCR

To examine the mRNA expressions of *Fcgr2b*, *Fcgr3*, and β-*actin*, total RNAs were obtained from the kidneys, spleens, and thymuses of 1- and 6-month-old C57BL/6 and B6.MRLc1(92–100) mice using TRIzol reagent (Invitrogen, Carlsbad, CA, USA). Purified total RNAs were treated with DNase for DNA digestion (Nippon Gene, Toyama, Japan) and cDNAs were synthesized using ReverTra Ace (Toyobo, Osaka, Japan) and Oligo-dT primer (Invitrogen). PCR for amplification was carried out with ExTaq (Takara, Tokyo, Japan) under the following conditions: 5 min at 95 °C, 35 cycles of 40 s at 95 °C, 30 s at 58 °C, and 30 s at 72 °C followed by 5 min at 72 °C. The details of the specific primers used for each gene are provided in Table 1.

Table 1 | Summary of gene-specific primer pairs

Genes (accession no.)	Primer sequence (primer position)	Products size
Fcgr2b (NM001077189.1)		
Forward	5′-CTGAGGCTGAGAATACGATC-3′ (1,000–1,019)	307 bp
Reverse	5′-GTGGATCGATAGCAGAAGAG-3′ (1,287–1,306)	
Fcgr3 (NM010188.4)		
Forward	5′-ATCACTGTCCAAGATCCAGC-3′ (652–671)	346 bp
Reverse	5′-GCCTTGAACTGGTGATCCTA-3′ (978–997)	
β-Actin (NM007393)		
Forward	5′-TGTTACCAACTGGGACGACA-3′ (304–323)	165 bp
Reverse	5′-GGGGTGTTGAAGGTCTCAAA-3′ (449–468)	

Quantitative real-time PCR analysis was performed using Brilliant SYBR Green QPCR Master Mix and real-time thermal cycler (MX 3000; Stratagene, Milano, Italy) to obtain cDNAs. The specific primers for each gene were the same as those used for reverse transcriptase-PCR. The amplification conditions were as follows: 10 min at 95 °C, 40 cycles of 10 s at 95 °C, 20 s at 58 °C, and 20 s at 72 °C, one cycle of 10 s at 95 °C, 20 s at 58 °C, and 20 s at 95 °C. ROX dye was included in each reaction to normalize non-PCR-related fluctuations in the fluorescence signals. The amplification specificity of all the PCR reactions was confirmed by melting-curve analysis. Non-template controls were included for each primer pair to assess any significant levels of contaminants. Quantitative data of *Fcgrs* were normalized to β-*actin* expression. The ratio of *Fcgr3* to *Fcgr2b* was calculated from these normalized values and expressed as fold increases compared with those of C57BL/6.

Statistical analysis

Results were expressed as mean ± s.e. and statistically analyzed by the non-parametric Mann-Whitney *U*-test ($P<0.05$).

DISCLOSURE

All the authors state no competing interests.

ACKNOWLEDGMENTS

This work was supported by grants from Research Fellowships of the Japan Society for the Promotion of Science for Young Scientists (no. 19000862) and the Ministry of Education, Culture, Sports, Science and Technology, Japan (no. 19380162).

REFERENCES

1. Santiago-Raber ML, Laporte C, Reininger L *et al.* Genetic basis of murine lupus. *Autoimmun Rev* 2004; **3**: 33–39.
2. Ichii O, Konno A, Sasaki N *et al.* Autoimmune glomerulonephritis induced in congenic mouse strain carrying telomeric region of chromosome 1 derived from MRL/MpJ. *Histol Histopathol* 2007; **23**: 411–422.
3. Ferluga D, Jerse M, Vizjak A *et al.* Correlation among WHO classes, histomorphologic patterns of glomerulonephritis and glomerular immune deposits in SLE. *Wien Klin Wochenschr* 2000; **112**: 692–701.
4. Hill GS, Delahousse M, Nochy D *et al.* Class IV-S versus class IV-G lupus nephritis: clinical and morphologic differences suggesting different pathogenesis. *Kidney Int* 2005; **68**: 2288–2297.
5. Hvala A, Kobenter T, Ferluga D. Fingerprint and other organised deposits in lupus nephritis. *Wien Klin Wochenschr* 2000; **112**: 711–715.

6. Takai T. Fc receptors and their role in immune regulation and autoimmunity. *J Clin Immunol* 2005; **25**: 1–18.
7. Takai T. Role of Fc gamma receptors in immune regulation and diseases. *Nihon Rinsho Meneki Gakkai Kaishi* 2005; **28**: 318–326.
8. Herrada AA, Contreras FJ, Tobar JA *et al.* Immune complex-induced enhancement of bacterial antigen presentation requires Fcγ receptor III expression on dendritic cells. *Proc Natl Acad Sci USA* 2007; **104**: 13402–13407.
9. Mechetina LV, Najakshin AM, Alabyev BY *et al.* Identification of CD16-2, a novel mouse receptor homologous to CD16/Fc gamma RIII. *Immunogenetics* 2002; **54**: 463–468.
10. Reth M. Antigen receptor tail clue. *Nature* 1989; **338**: 383–384.
11. Ravetch JV, Bolland S. IgG Fc receptors. *Annu Rev Immunol* 2001; **19**: 275–290.
12. Moser KL, Neas BR, Salmon JE *et al.* Genome scan of human systemic lupus erythematosus: evidence for linkage on chromosome 1q in African–American pedigrees. *Proc Natl Acad Sci USA* 1998; **95**: 14869–14874.
13. Shai R, Quismorio Jr FP, Li L *et al.* Genome-wide screen for systemic lupus erythematosus susceptibility genes in multiplex families. *Hum Mol Genet* 1999; **8**: 639–644.
14. Chu ZT, Tsuchiya N, Kyogoku C *et al.* Association of Fcγ receptor IIb polymorphism with susceptibility to systemic lupus erythematosus in Chinese: a common susceptibility gene in the Asian populations. *Tissue Antigens* 2004; **63**: 21–27.
15. Kyogoku C, Dijstelbloem HM, Tsuchiya N *et al.* Fcγ receptor gene polymorphisms in Japanese patients with systemic lupus erythematosus: contribution of FCGR2B to genetic susceptibility. *Arthritis Rheum* 2002; **46**: 1242–1254.
16. Siriboonrit U, Tsuchiya N, Sirikong M *et al.* Association of Fcγ receptor IIb and IIIb polymorphisms with susceptibility to systemic lupus erythematosus in Thais. *Tissue Antigens* 2003; **61**: 374–383.
17. Koene HR, Kleijer M, Swaak AJ *et al.* The FcγRIIIA-158F allele is a risk factor for systemic lupus erythematosus. *Arthritis Rheum* 1998; **41**: 1813–1818.
18. Wu J, Edberg JC, Redecha PB *et al.* A novel polymorphism of FcγRIIIa (CD 16) alters receptor function and predisposes to autoimmune disease. *J Clin Invest* 1997; **100**: 1059–1070.
19. Hatta Y, Tsuchiya N, Ohashi J *et al.* Association of Fcγ receptor IIIB, but not of Fc γ receptor IIA and IIIA, polymorphisms with systemic lupus erythematosus in Japanese. *Genes Immun* 1999; **1**: 53–60.
20. Bolland S, Ravetch JV. Spontaneous autoimmune disease in Fc (gamma) RIIB-deficient mice results from strain-specific epistasis. *Immunity* 2000; **13**: 277–285.
21. Clynes R, Dumitru C, Ravetch JV. Uncoupling of immune complex formation and kidney damage in autoimmune glomerulonephritis. *Science* 1998; **279**: 1052–1054.
22. Matsumoto K, Watanabe N, Akikusa B *et al.* Fc receptor-independent development of autoimmune glomerulonephritis in lupus-prone MRL/lpr mice. *Arthritis Rheum* 2003; **48**: 486–494.
23. Takai T, Ono M, Hikida M *et al.* Augmented humoral and anaphylactic responses in FcγRII-deficient mice. *Nature* 1996; **379**: 346–349.
24. He X, Schoeb TR, Panoskaltsis-Mortari A *et al.* Deficiency of P-selectin or P-selectin glycoprotein ligand-1 leads to accelerated development of glomerulonephritis and increased expression of CC chemokine ligand 2 in lupus-prone mice. *J Immunol* 2006; **177**: 8748–8756.
25. Ito MR, Ono M, Itoh J *et al.* Bone marrow cell transfer of autoimmune diseases in a MRL strain of mice with a deficit in functional Fas ligand: dissociation of arteritis from glomerulonephritis. *Pathol Int* 2003; **53**: 518–524.
26. Namiki Y, Kon Y, Kazusa K *et al.* Quantitative trait loci analysis of heat stress resistance of spermatocytes in the MRL/MpJ mouse. *Mamm Genome* 2005; **16**: 96–102.
27. Floege J, Radeke HR, Johnson RJ. Glomerular cells *in vitro* versus the glomerulus *in vivo*. *Kidney Int* 1994; **45**: 360–368.
28. Radeke HH, Meier B, Topley N *et al.* Interleukin 1-alpha and tumor necrosis factor-alpha induce oxygen radical production in mesangial cells. *Kidney Int* 1990; **37**: 767–775.
29. Fukami K, Ueda S, Yamagishi S *et al.* AGEs activate mesangial TGF-beta-Smad signaling via an angiotensin II type I receptor interaction. *Kidney Int* 2004; **66**: 2137–2147.
30. Hora K, Satriano JA, Santiago A *et al.* Receptors for IgG complexes activate synthesis of monocyte chemoattractant peptide 1 and colony-stimulating factor 1. *Proc Natl Acad Sci USA* 1992; **89**: 1745–1749.
31. Radeke HH, Janssen-Graalfs I, Sowa EN *et al.* Opposite regulation of type II and III receptors for immunoglobulin G in mouse glomerular mesangial cells and in the induction of anti-glomerular basement membrane (GBM) nephritis. *J Biol Chem* 2002; **277**: 27535–27544.
32. Desai DD, Harbers SO, Flores M *et al.* Fc gamma receptor IIB on dendritic cells enforces peripheral tolerance by inhibiting effector T cell responses. *J Immunol* 2007; **178**: 6217–6226.
33. Regnault A, Lankar D, Lacabanne V *et al.* Fc γ receptor-mediated induction of dendritic cell maturation and major histocompatibility complex class I-restricted antigen presentation after immune complex internalization. *J Exp Med* 1999; **189**: 371–380.
34. Boruchov AM, Heller G, Veri MC *et al.* Activating and inhibitory IgG Fc receptors on human DCs mediate opposing functions. *J Clin Invest* 2005; **115**: 2914–2923.
35. Radeke HH, Resch K. The inflammatory function of renal glomerular mesangial cells and their interaction with the cellular immune system. *Clin Invest* 1992; **70**: 825–842.
36. Radeke HH, Emmendörffer A, Uciechowski P *et al.* Activation of autoreactive T-lymphocytes by cultured syngeneic glomerular mesangial cells. *Kidney Int* 1994; **45**: 763–774.
37. Durum SK, Lee CK, Geiman TM *et al.* CD16 cross-linking blocks rearrangement of the TCR beta locus and development of alpha beta T cells and induces development of NK cells from thymic progenitors. *J Immunol* 1998; **161**: 3325–3329.
38. Xiu Y, Nakamura K, Abe M *et al.* Transcriptional regulation of *Fcgr2b* gene by polymorphic promoter region and its contribution to humoral immune responses. *J Immunol* 2005; **169**: 4340–4346.
39. Blank MC, Stefanescu RN, Masuda E *et al.* Decreased transcription of the human FCGR2B gene mediated by the -343 G/C promoter polymorphism and association with systemic lupus erythematosus. *Hum Genet* 2005; **117**: 220–227.
40. Fujii T, Hamano Y, Ueda S *et al.* Predominant role of Fc gamma RIII in the induction of accelerated nephrotoxic glomerulonephritis. *Kidney Int* 2003; **64**: 1406–1416.
41. Mold C, Gresham HD, Du Clos TW. Serum amyloid P component and C-reactive protein mediate phagocytosis through murine FcγRs. *J Immunol* 2001; **166**: 1200–1205.
42. Bickerstaff MC, Botto M, Hutchinson WL *et al.* Serum amyloid P component controls chromatin degradation and prevents antinuclear autoimmunity. *Nat Med* 1999; **5**: 694–697.
43. Du Clos TW, Zlock LT, Hicks PS *et al.* Decreased autoantibody levels and enhanced survival of (NZBxNZW) F1 mice treated with C-reactive protein. *Clin Immunol Immunopath* 1994; **70**: 22–27.
44. Haywood ME, Rose SJ, Horswell S *et al.* Overlapping BXSB congenic intervals, in combination with microarray gene expression, reveal novel lupus candidate genes. *Genes Immun* 2006; **7**: 250–263.
45. Rozzo SJ, Allard JD, Choubey D *et al.* Evidence for an interferon-inducible gene, *Ifi202*, in the susceptibility to systemic lupus. *Immunity* 2001; **15**: 435–443.